5th International Conference on
New Developments In Photo-Detection 2008

Palais des Congrès, Aix-les-Bains, France, June 15-20, 2008

Highlights of Poster Session I

Thierry Gys
CERN – Geneva – Switzerland

Poster Session I – details

- 25 contributions (originally 27 - 2 withdrawn)
- Covered technologies and fields are:
  - Avalanche and PIN photo-diodes – 8 contributions
  - CMOS and CT detectors – 3 contributions
  - Gaseous detectors – 5 contributions
  - Vacuum photo-detectors (PMTs, HPDs, MCPs) – 9 contributions
  - Some overlap

Acknowledgments and disclaimer

- Many thanks to (almost) all contributors for their highlight slides!
- Very helpful material, sometimes complemented by previous literature on the same subject
- Order of presentation is numerical – no preference!
- Apologies for possible (probable) inconsistencies – be tolerant!

Avalanche and PIN photo-diodes

8 contributions

Prototype and mass production tests of Avalanche Photo Diodes for the Electromagnetic Calorimeter in the ALICE experiment at LHC – F. Riggi et al. – P027

- **ALICE EMcal design**
  - Coverage: $|\eta|<0.7$, $\Delta\Phi = 110°$
  - Lead-scintillator sampling calorimeter - Shashlik fiber geometry
  - APD readout (13k)

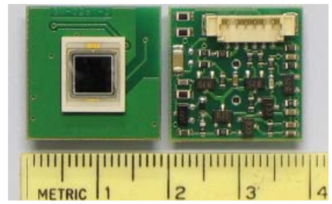

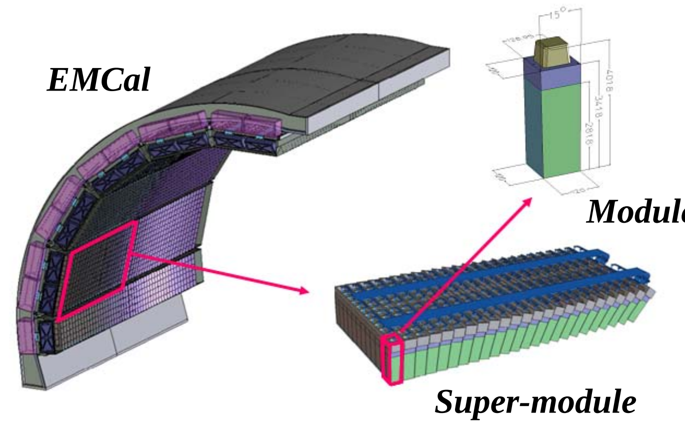

- **Test procedure**
  - Selecting APDs according to their performance
  - Measuring the APD gain dependence on the bias voltage (Voltage Coefficient dM/dV × 1/M)
  - Evaluating the nominal voltage setting for the APD to obtain gain M=30
  - Measuring the APD gain dependence on the operating temperature (Temperature Coefficient dM/dT × 1/M)

M vs bias voltage

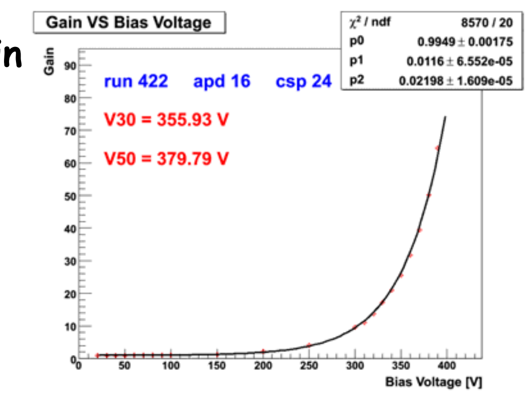

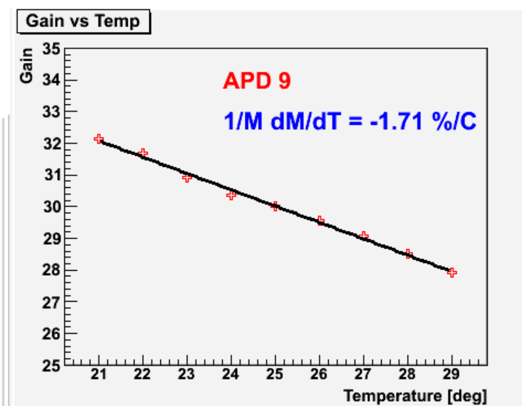

1/M x dM/dT vs T

Application of Simple Negative Feedback model for Avalanche Photo Detectors investigation – V. Kushpil – P046

- **APD model**
  - Derivations from Miller's gain formula: APD ~ system w. negative feedback B
  - Results in 4 behaviour types
    - B=0 no negative FB
    - K>0 FB rise slower than gain rise – unstable operation
    - K=0 FB rise equal to gain rise – stable
    - K<0 FB rise faster than gain rise – stable
- **Experimental results**
  - B found from difference between experimental and simulated values of 1/M(V)
  - K and B found as sensitive variables useful for description of APD gain behavior
  - The model also describes dynamics features of the APD response

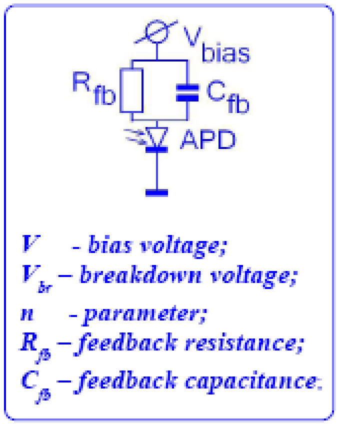

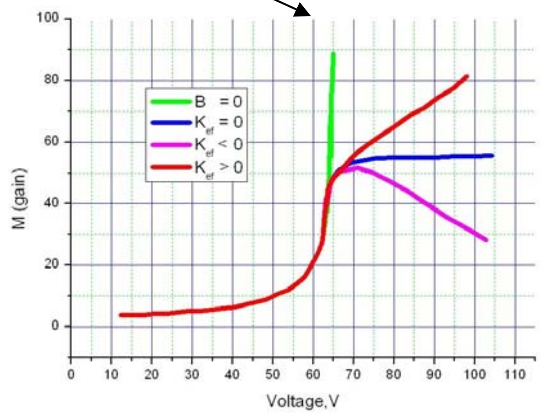

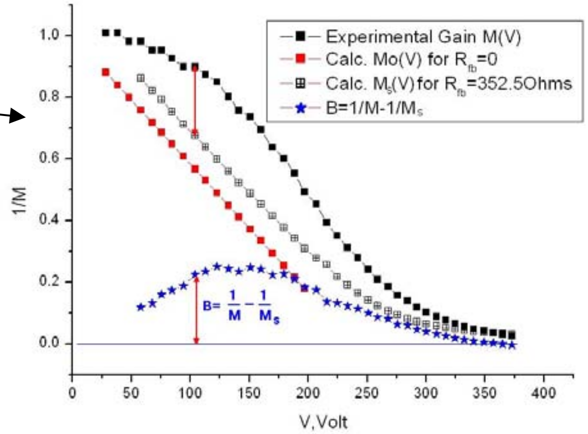

A Study of deep diffused, low resistivity, silicon avalanche photodiode coupled to a $LaBr_3$:Ce scintillator
M. McClish et al. – P062

- **Motivations**
  - Improved spectroscopic performance
  - New APD fabrication process, using lower ρ Si
- **Performance**
  - QE has improved by ~ 2 across the emission range for LaBr3:Ce
  - Noise has decreased by ~ 4 for the same area and temperature
  - Using $LaBr_3$:Ce, the energy resolution is 2.55% (FWHM) at 662 keV! Comparable to CZT The resolution from $LaBr_3$:Ce coupled to PMT is 3.0%

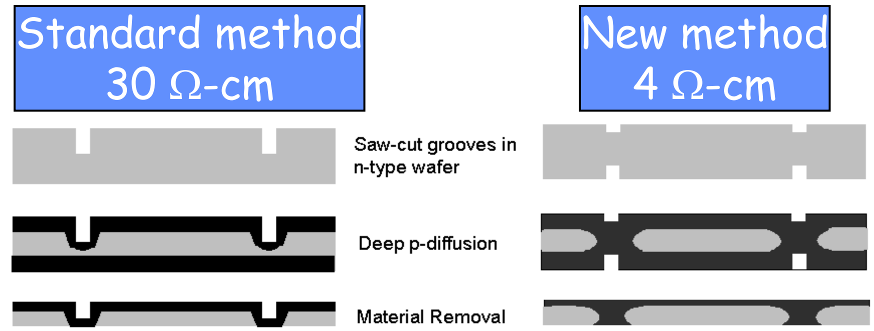

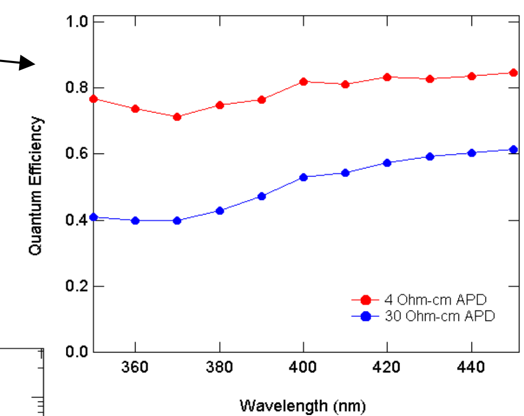

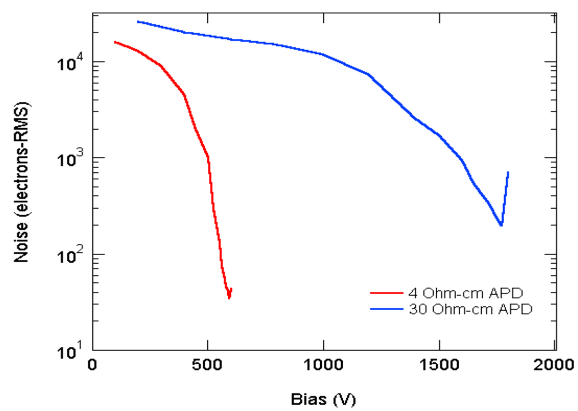

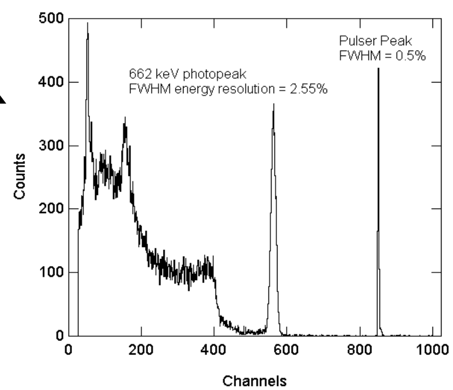

An alternative to silicon-based sensors for single photon detection at 1064nm – A. Rochas et al. – P069

- **Single-photon detector combining:**
  - InGaAsP/InP APD
    - InGaAsP quaternary absorber optimized for 1064nm
    - InP multiplication layer
    - 3-stage TEC integrated in TO8 (down to -50°C)
    - free-space
  - Integrated pulser
    - Chip area: 1.6mm^2
    - 0.8μm CMOS technology
    - Supply voltage VDD=+5V
- **Performance**
  - Dark Count Rate
    - <60Hz @ det. prob. of 7.5%, <400Hz @ 15%, <2.5kHz @ 30%

    @ - 40°C, 80μm ∅ APD
  - Afterpulsing
    - <1% @ det. prob. of 7.5% and 20μs dead time, <3% @ 15% and 20μs, <5% @ 30% and 50μs
  - Single pe det. prob.
    - up to 30% at 1064nm
    - spectral range [900,1200nm]
  - Timing resolution
    - <150ps

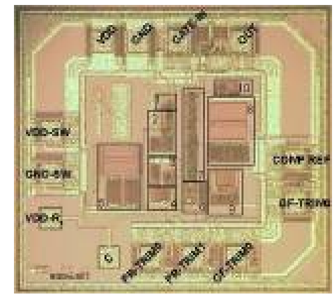

DCR vs Excess Bias Voltage

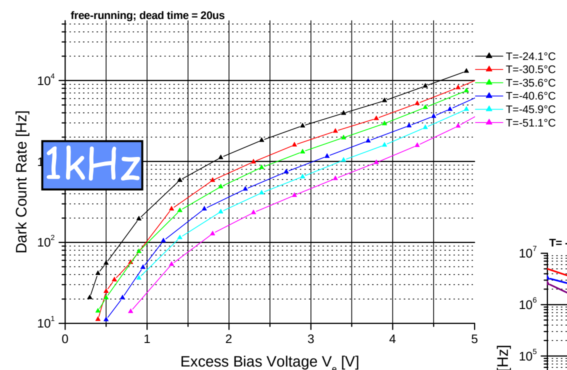

DCR vs Dead Time

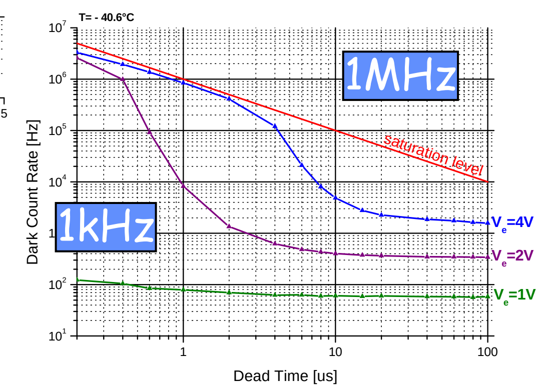

A design for a linear array PIN photodiode for use in a Computed mammo-Tomography (CmT) System
S.-W. Park – P085

- **Motivations**
  - CmT using a fan-beam type X-ray source and PD linear array
  - Optimize sensitivity in wavelength range 450-700nm (peak 510nm) for Gd_2O_2S (GOS) crystal light detection
  - Make p-layer as shallow as possible

Fan-beam CmT schematic design

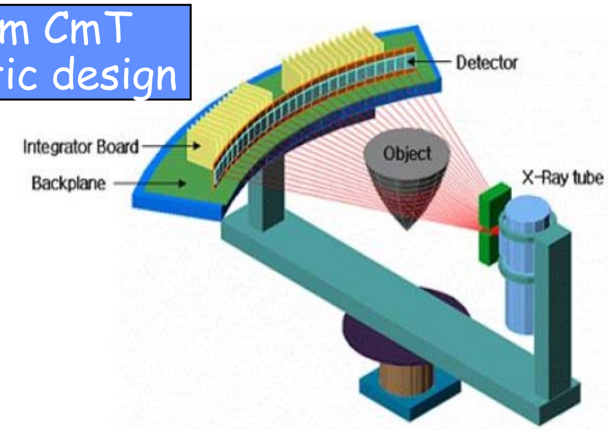

Photo sensitivity vs wavelength

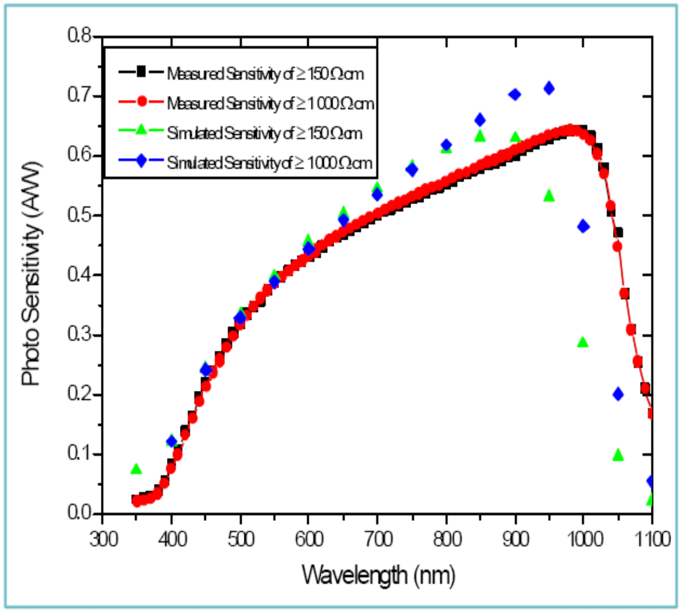

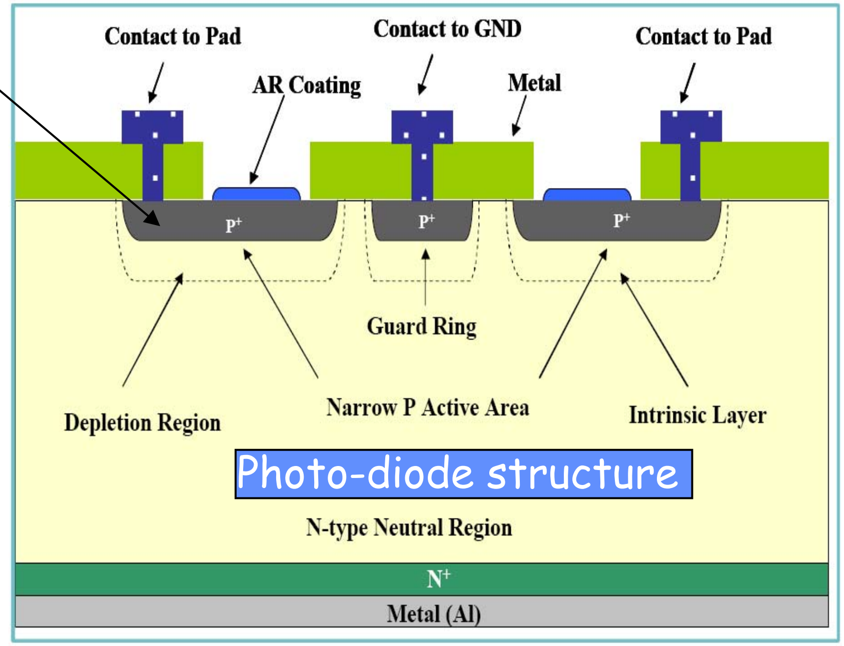

Detection of scintillation light from $Pr:Lu_3Al_5O_{12}$(LuAG) by Gallium nitride photodiode – K. Kamada et al. – P090

- **Motivations**
  - Detection of UV scintillation light from Pr:LuAG (Praseodymium-doped) by a InGaN-PD photo-detector
- **Pr:LuAG scintillator**

  - UV emission
  - Good energy resolution
  - Fast decay time

	Pr:LuAG	Ce:GSO	Ce:LYSO	BGO
Energy resolution (%@662keV)	4.6%	8%	8%	10%
Light yield (ph/MeV)	18000	12500	33000	8000
Decay time (ns)	20	40~60	40	300
Emission wavelength (nm)	310	430	420	480

- **InGaN-PD photo-detector**

  - High sensitivity in UV

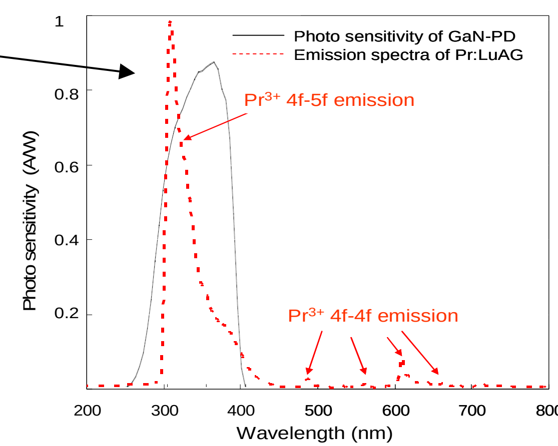

- **Results**
  - 5.5MeV α-ray peak (^{241}Am) clearly detected
  - Energy resolution ~ 29%
  - Applications in radiation detection

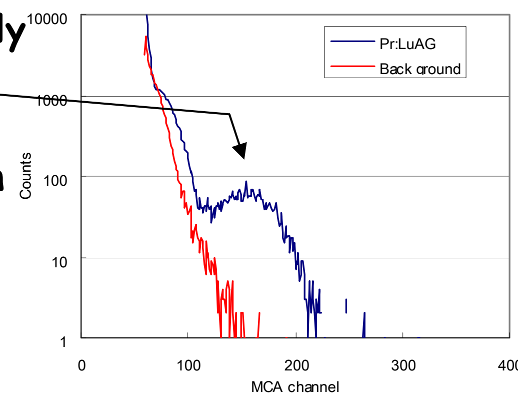

Digital electronics for PSAPD-based Gamma Cameras
Materials and Methods – A. Fallu-Labruyère – P194

Motivations

- Characterize Position-Sensitive Avalanche photodiode performance wrt size and operating temperature
- Use light pulser and CsI(Tl) crystal arrays
- Use coincidence digital spectrometer DGF-Pixie-4

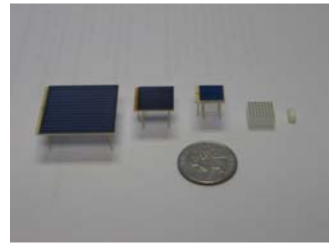

Results

- Position resolution of 2.2mm±0.2mm measured with 28x28 mm^2 devices cooled at -32°C
- Digital electronics easily scalable and well suited for larger field-of-view gamma cameras (detector tiling instrumentation).

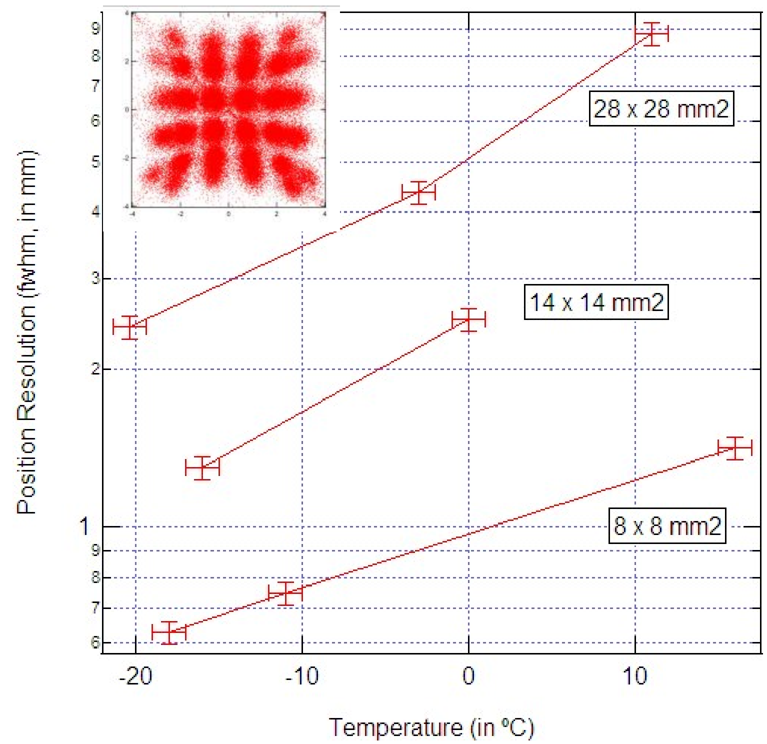

Position resolution versus device size and temperature (140keV, 100ns peaking time)
Upper corner: flood exposure, -20°C, CsI(Tl) array 1.35mm pitch, 8x8 mm^2 PSAPD

CMOS and CT detectors

3 contributions

A method to remove the projection error in triple-energy radiography with contrast medium – N. Lanconelli – P071

- **Motivations**
  - Multi-energy CT
  - Quasi-monochromatic X-ray beams with energy 20-70keV
  - Triple-energy radiography results in projection errors 10 to 60 times smaller, with respect to the dual-energy errors
- **Results**

28 keV | 36 keV | 44 keV

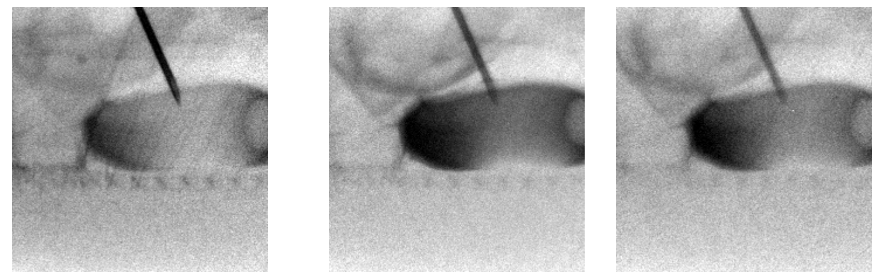

Monochromatic images

Dual-energy

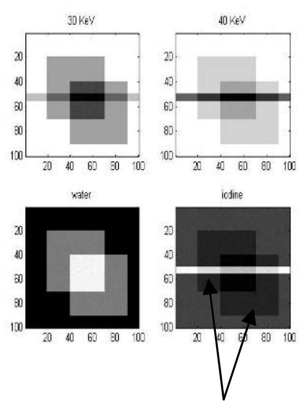

Projection errors

Triple-energy

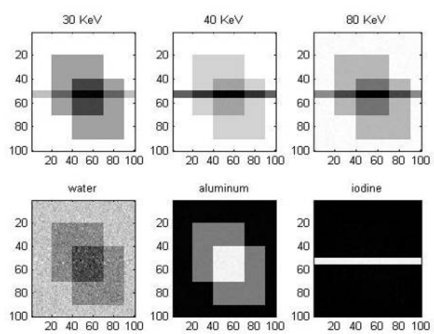

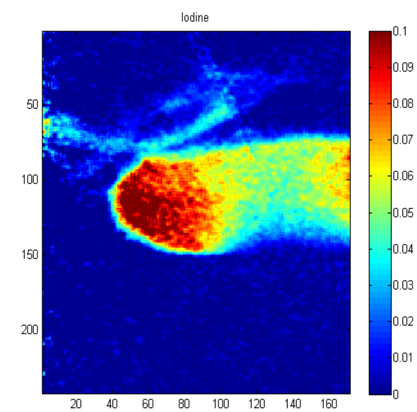

Reconstructed Iodine image

(mass-thickness map)

Ionization versus displacement damage effects in proton irradiated CMOS sensors manufactured in deep submicron process – V. Goiffon et al. – P108

- **Motivations**
  - Study of proton irradiation effects on CMOS sensors manufactured in a deep submicron technology dedicated to imaging applications
- **Test chip**
  - 0.18 μm CMOS CIS technology
  - Shallow trench isolations (STI), dedicated photodiode doping profiles
  - 128 x 128 pixel array, 3T, 10μm pitch
  - Larger photodiodes (>10^4 μm²), others tests structures (MOSFET)
- **Proton irradiation**
  - Facilities : KVI, UCL, Isotron
  - Energies : 7.4 to 200 MeV
  - Fluences : 5 x 109 to 3 x 1011 H+/cm²
- **Results**
  - No photo-response degradation, no voltage shift, no gain reduction
  - Ionization-induced dark current increase is the main degradation
  - Displacement damages still play a significant role in uniformity degradation

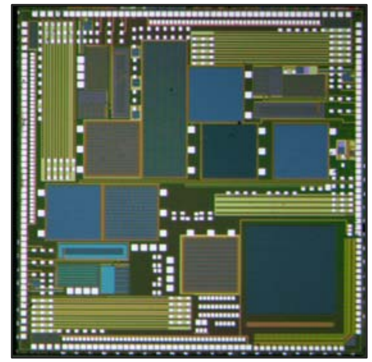

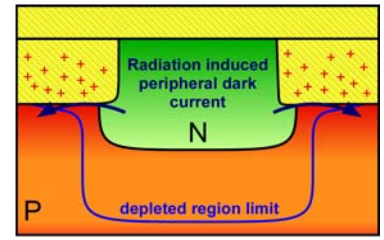

Dark current increase vs. ionizing dose

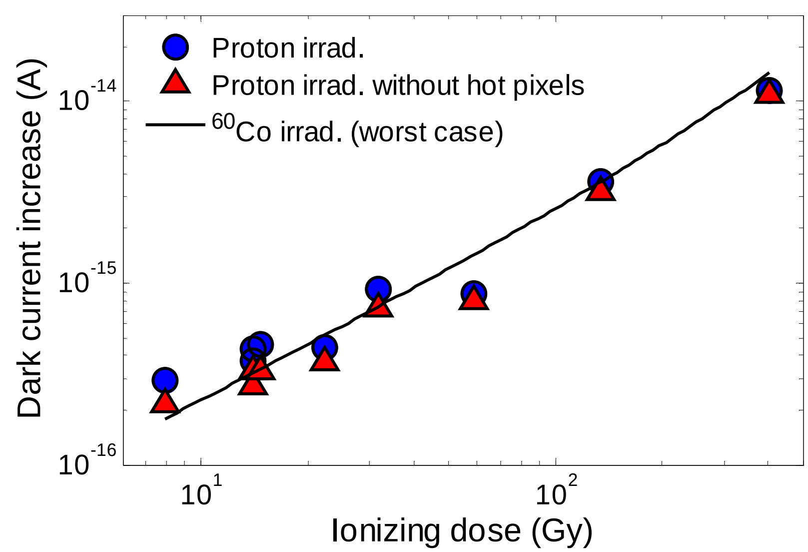

High-Performance Imagers for Space Applications: the Strong Benefits of CMOS Image Sensor Processes
O. Saint-Pe et al. – P162

- **Motivations**
  - Moving forward by using available CMOS image sensor processes to build high electro-optics performance image sensors dedicated to space applications
- **First Operational Application**
  - Earth spectral imaging on geostationary orbit - launch at end of 2008
  - 2M pixels 2D array, 3T photo-diodes, 11x14 μm^2 pitch, 0.35 μm CMOS CIS technology
  - High QE and MTF, low dark current
- **Second Application**
  - EC & ESA Sentinel 2 program in low Earth orbit - launch in 2012
  - Multi-linear detector with 10 photodiodes rows, 7.5 and 15 μm pitch
  - 12 Detectors per Focal Plane, 250 mm length, 290 km Swath with 10 and 20 m resolutions
- **Upstream Programs & Perspectives**
  - Sensitivity Improvement
  - Reduced Pitch / Higher Density
  - Read Out Noise Reduction
  - On Chip Signal Processing

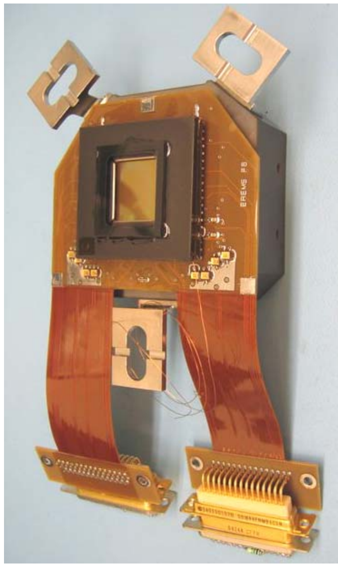

MTF vs wavelength

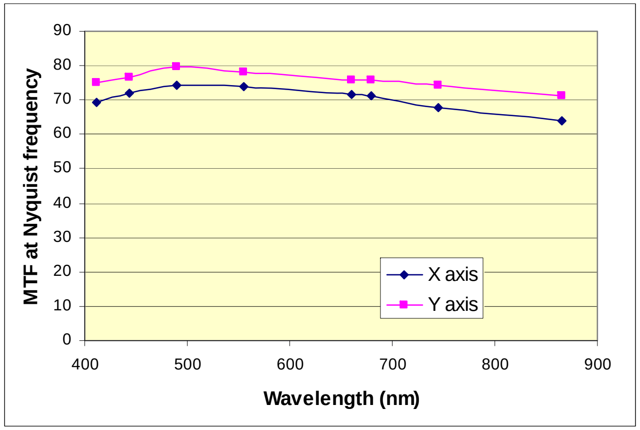

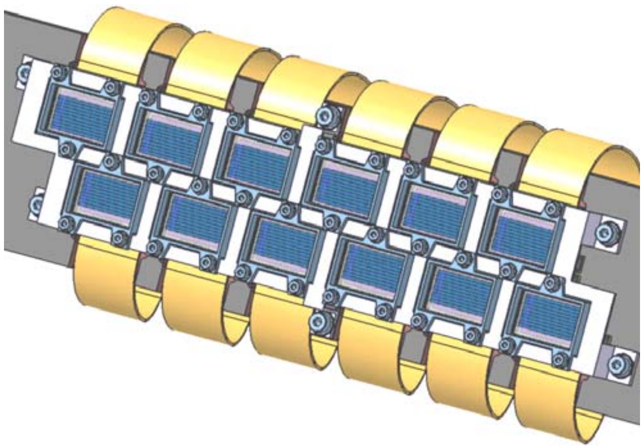

Gaseous detectors

5 contributions

Photoelectron Backscattering in Ar-CF_4 and Xe-CF_4 gaseous mixtures - J. Matias-Lopes et al. – P120

- ***Achieved results***
  - CE *f* studied for photoelectrons emitted from a CsI photocathode irradiated with a Hg(Ar) lamp (185nm centered, 5nm FWHM)
  - Ar-CF_4 and Xe-CF_4 mixtures studied as a function of CF_4 concentration
  - Reduced electric fields E/p: 0.1, 0.3, 1.0 and 2.6 V cm^{-1} $Torr^{-1}$, where p is the gas pressure
  - Dashed curves represent the corresponding CH_4 based mixtures

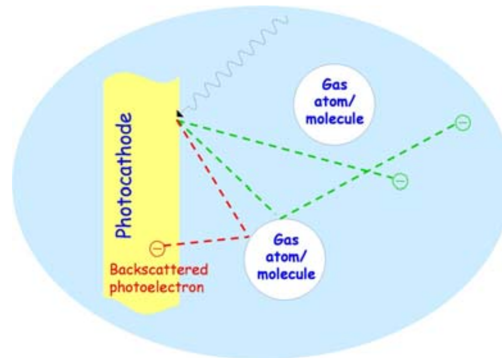

Addition of CH_4 or CF_4 to noble gases efficiently increases photoelectron transmission and drift velocity, due to the important role played by the vibrational excitation of the molecules at low electron impact energies

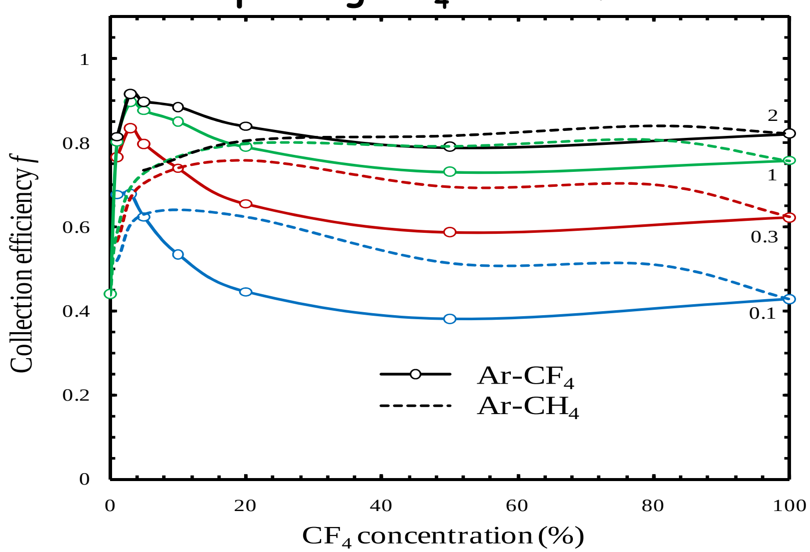

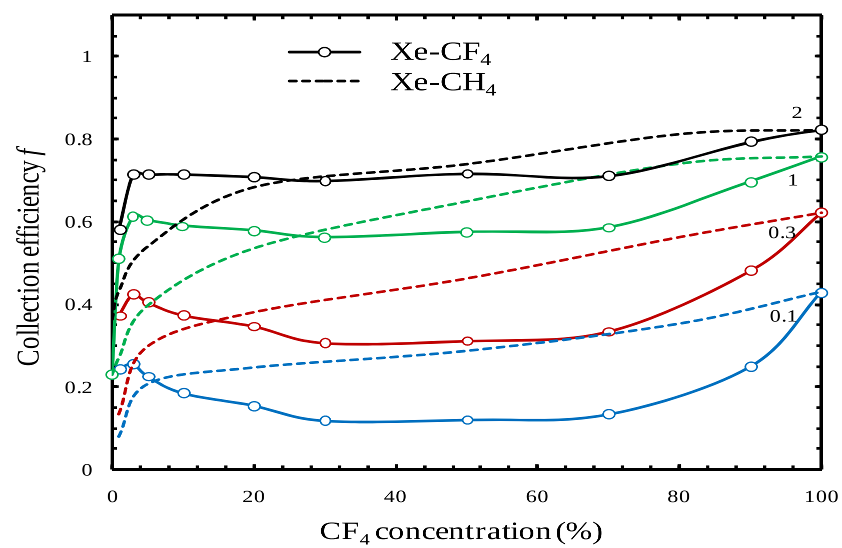

Influence of the substrate surface texture on the stability of CsI thin film photocathodes - M.-A. Nitti et al. – P168

- **CsI photo-cathodes**
  - hygroscopicity
  - stability of photoemission properties influenced by surface morphology
  - film growth in separate islands ⇒ no structural change after exposure to moisture

QE(24h)/QE(0h) vs wavelength

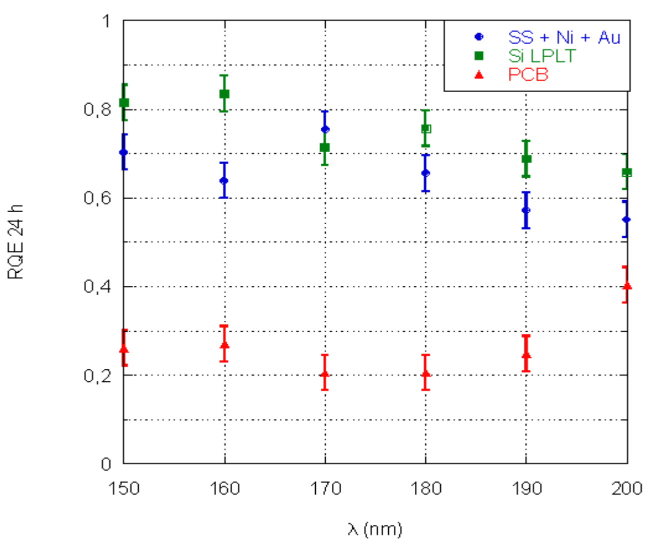

Patterning of conductive substrates by colloidal lithography

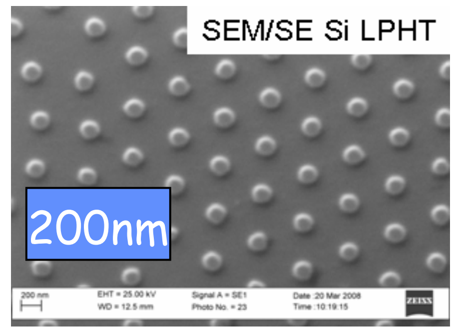

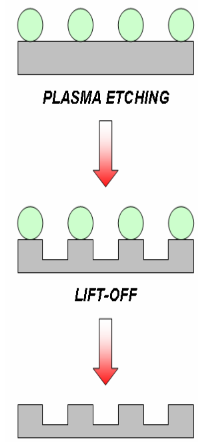

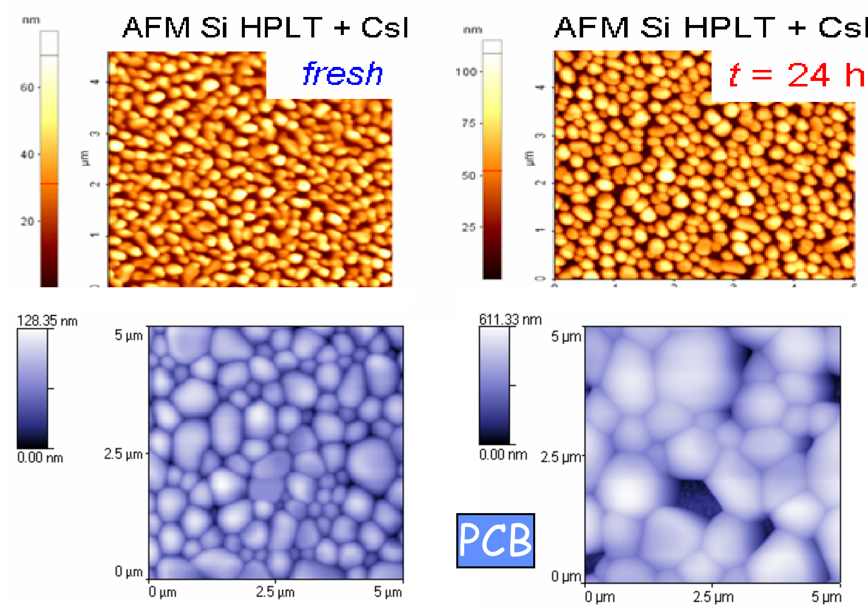

Ar-Xe mixtures and their use in curved grid gas proportional scintillation counters for X-rays - S. do Carmo et al. – P177

- **Gas Proportional Scintillation Counters**
  - competitive with solid-state based detectors when large detection areas are required and for soft X-ray detection.
  - very short (a few 100μm) L_a in pure Xe for soft X-rays ⇒ loss of primary electrons to the detector window by backscattering
  - Ar-Xe mixtures: longer L_a, similar scintillation yields, improved Fano factor F and w values.
- **Achieved results for each Ar-Xe mixture**
  - energy resolution
  - scintillation yield
  - thresholds for scintillation and ionization
  - spectra distortion minimized by « curve grid technique » shown to be gas-independant

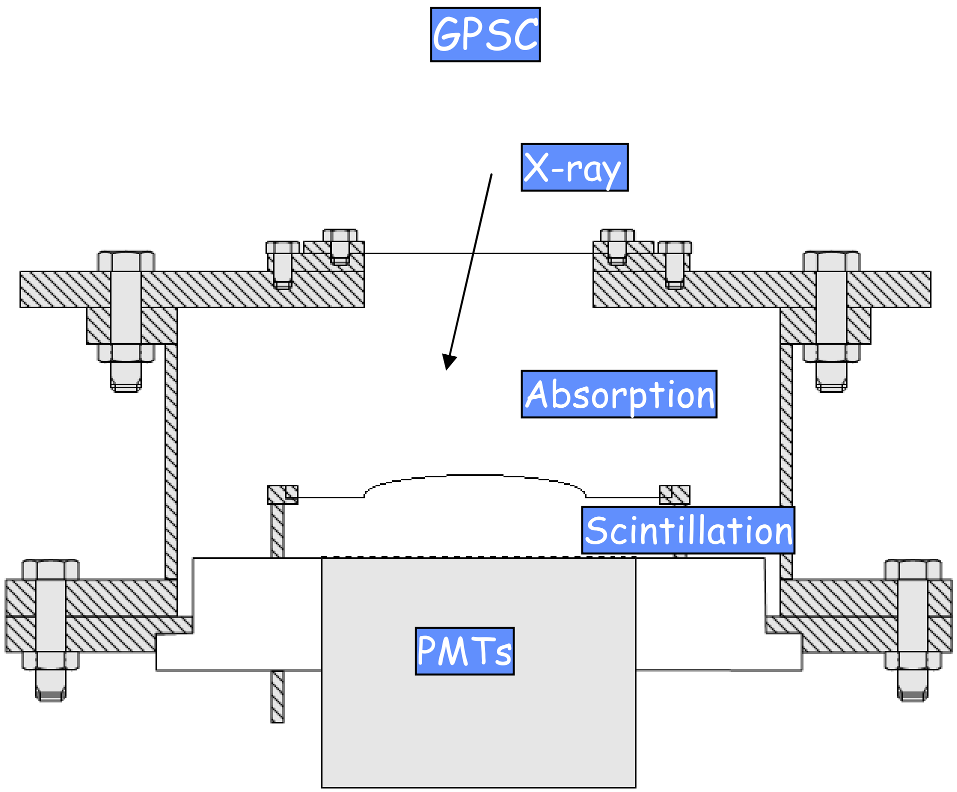

Gas VUV Photo-sensors Operating Face-to-Face
J. Veloso et al. – P196

- **CsI-MHSP photo-sensor for γ-ray detection**
  - Micro-Hole and Strip Plates coated with a 500nm CsI film)
  - High gains > 10^4 @ 1bar Xe
  - Fast charge collection – tens of ns
  - High rate capability > photons MHz/mm2
  - 2-D intrinsic capability – σ~125μm (with resistive line)
- **Performance**
  - Good position detection between both photo-sensors
  - Fair photoelectron collection – independent of gas pressure (up to 5 bar of Xe)
  - Vertical z position almost independent on the photon energy
  - Future work: 3D detection (z,x,y); add a small quantity of CF_4 to Xe to increase photoelectron collection efficiency

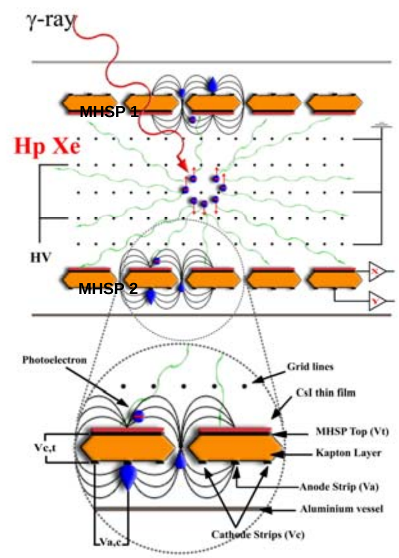

VUV scintillation from HpXe
- gamma absorption produce electrons
- electron drift between meshes induces secondary scintillation
- VUV photons reach both photo-sensors

Measured vs real position for 0.5mm collimated 60keV γ-rays Deviation <0.35mm

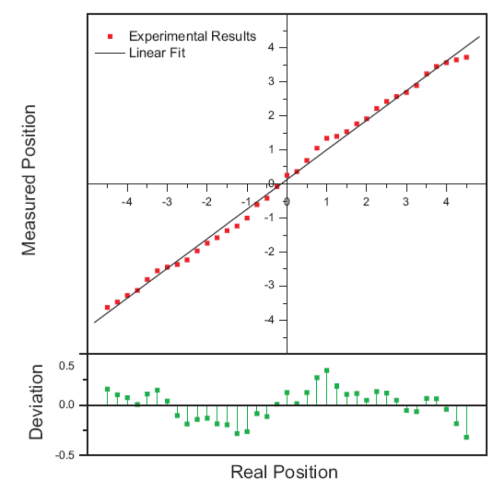

NDIP 2008

NDIP 2008

Vacuum photo-detectors (PMTs, HPDs, MCPs)

9 contributions

Investigation of ion feedback after-pulse spectra by the autocorrelation method - V. Morozov et al. – P055

- **Motivations**
  - Study AP time and charge distributions for various PMTs
  - Establish criteria for selection of PMTs with low AP rate
- **Principle of operation**
  - Based on autocorrelation method
  - Time range: up to 8µs
  - Use blue and red lights: AP time dependence clearly seen
  - Focussing potential distribution plays essential role
  - Two-stage autocorrelation spectrometer allows for the registration of a second AP (SAP) in the time range chosen for the registration of the first AP (FAP).

Block-diagram

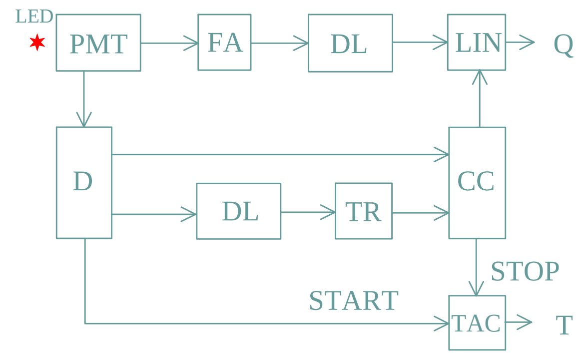

Time-diagram

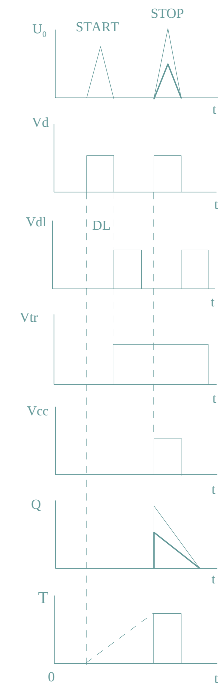

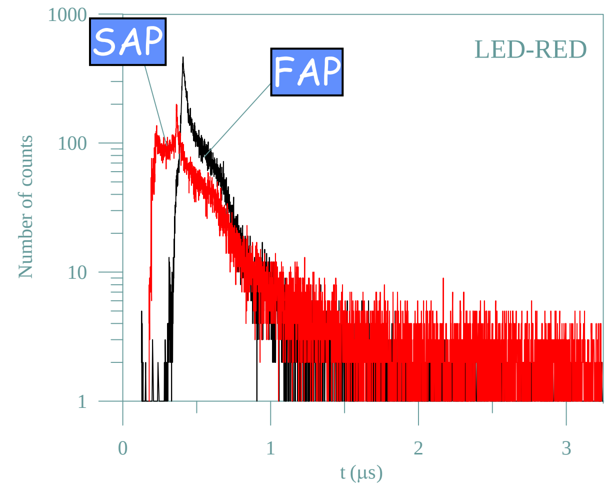

Time distributions of FAP and SAP for the XP2020 PMTc

Advances in Anodic Alumina MCP development
G. Drobychev et al. – P063

- **Anodic alumina oxide (AAO)**
  - Alternative to standard lead-silicate-glass MCP manufacturing
  - See NDIP05 for preliminary results
  - A technology to increase AAO electric conductivity was developed
  - New samples: R around tens of MΩ. The resistivity can be varied in a wide range, depending on the technological production parameters
  - An etching technology, which has a characteristic "anisotropy" due to porous structure of the AAO is also developed
  - Produced channels are open-ended and have constant diameter along the full depth of a plate. However, a technology optimization is still required
  - Plans to reach 150-180 µm MCP thickness while maintaining MCP structure parameters

SEM images

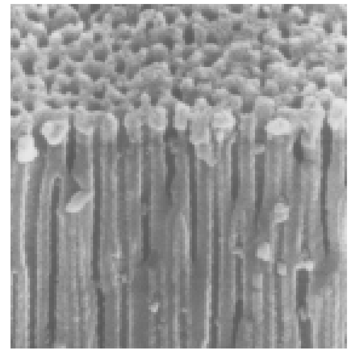

Natural AAO

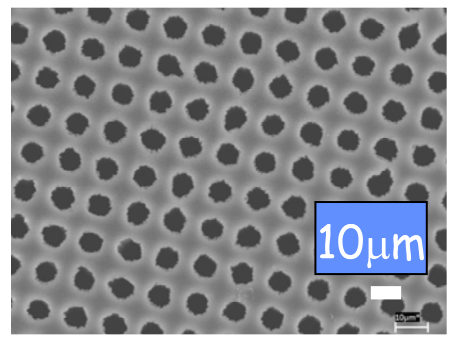

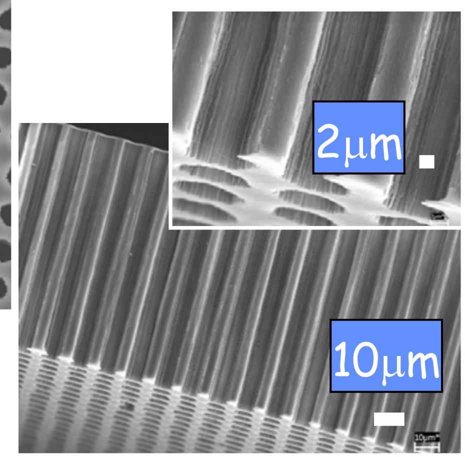

Etched AAO MCP samples

PMm²: A R&D on a triggerless acquisition for next-generation neutrino experiments - B. Genolini et al. – P093

- **Next-generation MT-scale water tanks**
  - very large surfaces of photo-detection and large data volume
- **PMm² R&D project**
  - Triggerless data acquisition (no possible local coincidence)
  - Replace large 20" PMTs by 12" (cheaper)
  - Modular design (assembly by 16 PMTs)
  - Underwater front-end electronics (less cables)
- **R&D organization**
  - ASIC development
  - 10b-resistant 12" PMT
  - 100m-long cable, surface controller
  - Water tightness, mechanics
  - 16-PMT demonstrator to be installed end 2009

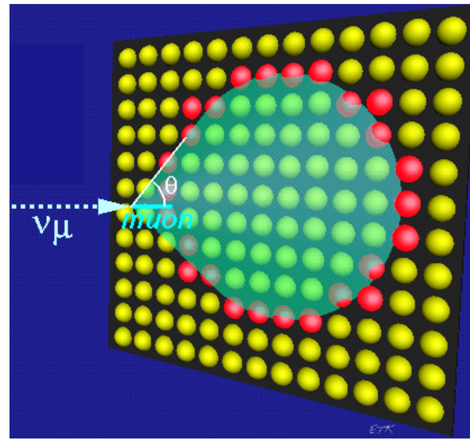

PMm²

http://pmm2.in2p3.fr

100m cable

Offline processing
(on the surface):
- Coincidence
- Noise rejection
- Trajectory reconstruction

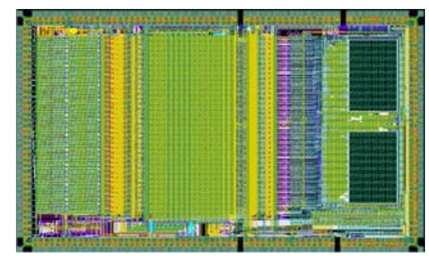

PARISROC:
-16 independent channels
-Analog processing + digitization
-Charge: 1 to 300 photoelectrons
-Time: 1 ns resolution FWHM

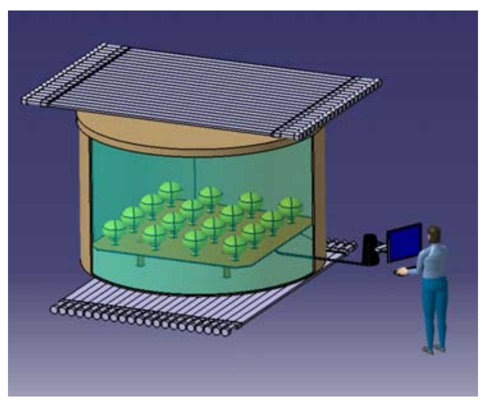

Investigation of the Secondary Emission Characteristics of CVD Diamond Films for Electron Amplification
J. Lapington et al. – P110

- **CVD Diamond dynode advantages**
  - Negative electron affinity - high secondary electron yield
  - Tight electron energy dist^{n} and low dynode count – excellent time resolution
  - Good gain statistics – low noise
  - Wide band-gap – low noise
  - Robust, stable SEY
  - Easy to manufacture – CVD
  - Boron doped – conductive
  - Easily patterned and structured
  - Promising for photon imagers – an array of MicroPMTs

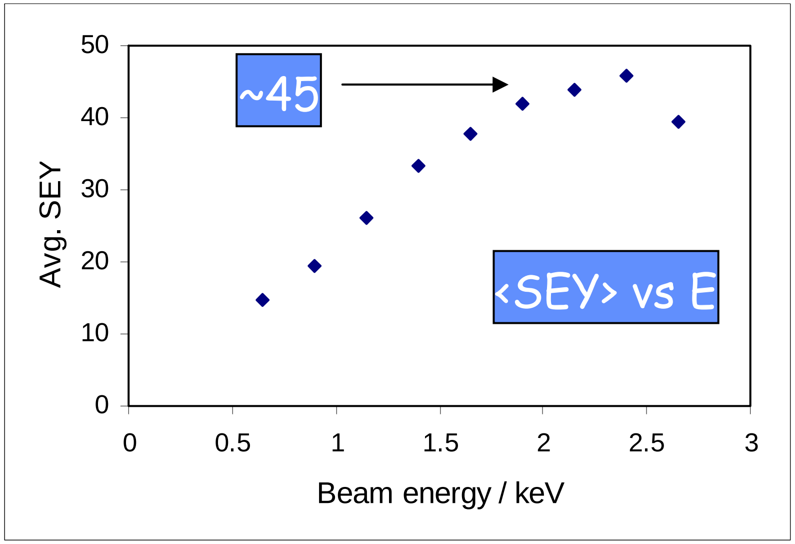

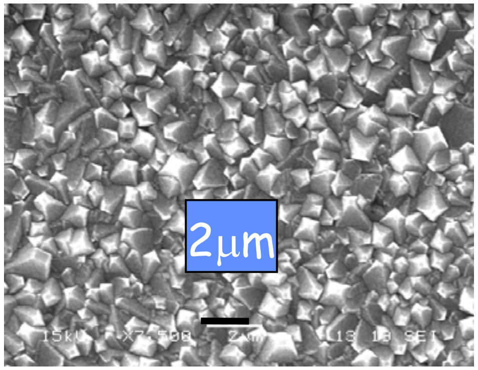

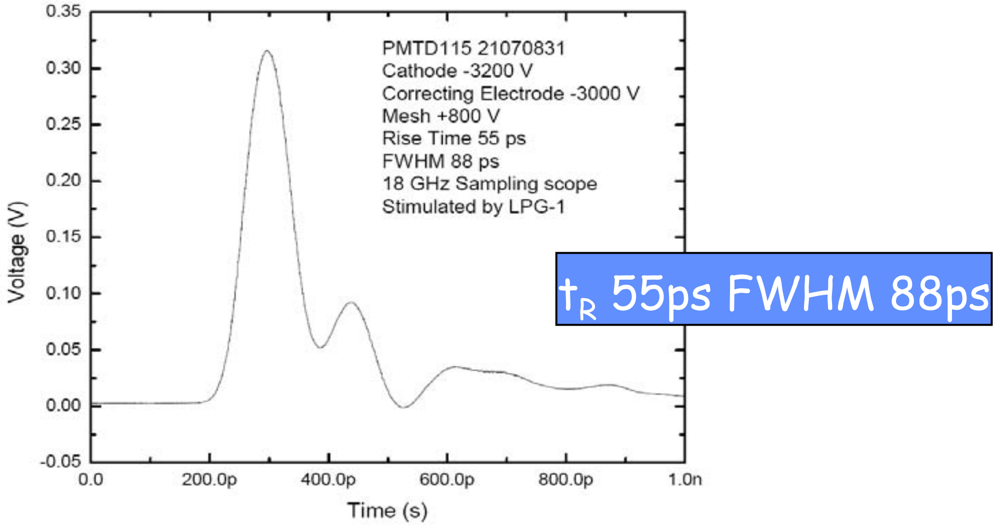

Scintillating Crystal Hybrid Photon Detector (X-HPD) development for the KM3NeT km³-scale neutrino telescope
G. Hallewell – P136

- **KM3Net**
  - Future deep-sea neutrino telescope with a >1km³ volume
  - « Offspring » of ANTARES, NEMO and NESTOR
  - Good angular resolution for μ, E_ν>10TeV, E_T a few 100GeV
  - Sensitive to all ν flavours and neutral-current reactions
- **X-HPD advantages**
  - High E-field:
    - <1ns TTS
    - insensitive to Earth's B-field
    - photon counting
  - Spherical PC:
    - ~100% CE over 3π
    - Double PC effect
    - Overall ε >35% (16-23% for hemispherical PMTs)
  - Increase Č photon horizon and instrumentable sea water volume
- **8" Photonis prototype tests**
  - Currently with metal anode

Photonis - Baikal - CERN

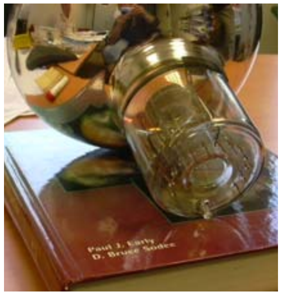

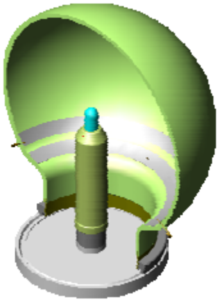

Effective Sν vs Eν

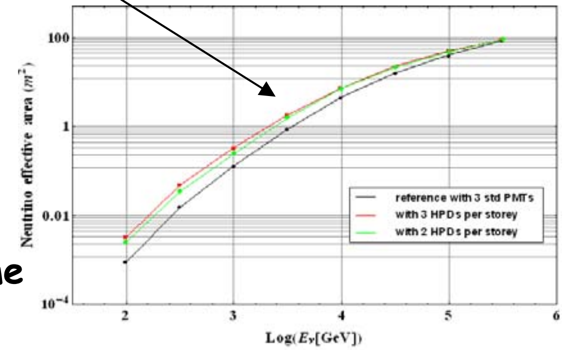

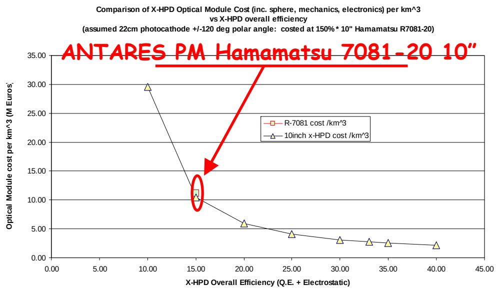

Cost vs X-HPD efficiency

PMT Selection for the MAGIC II Telescope
Ching-Cheng Hsu – P203

- **MAGIC I telescope**
  - Gamma-ray astronomy at low energies (<70GeV threshold) with high sensitivity
  - Search for eg Active Galactic Nuclei
  - MAGIC I: 236 m^2 single Imaging Atmosphere Cherenkov Telescope (IACT)
  - Magic II upgrade towards lower energies
- **PMT requirements**
  - High QE and DQE
  - Low gain $2\text{-}5\times10^4$ (ageing)
  - Low afterpulse rate
  - Good resolution
- **Tests of 25 PMTs from 2 manufacturers**
  - Performance comparable
  - Better QE for Hamamatsu

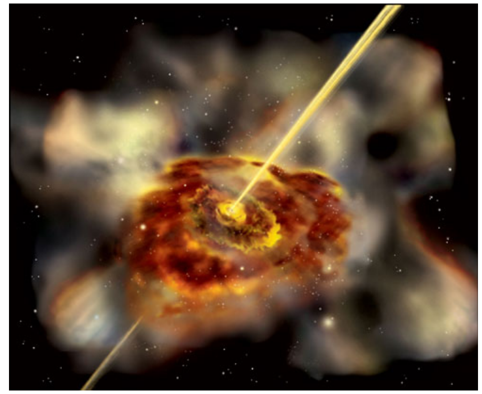

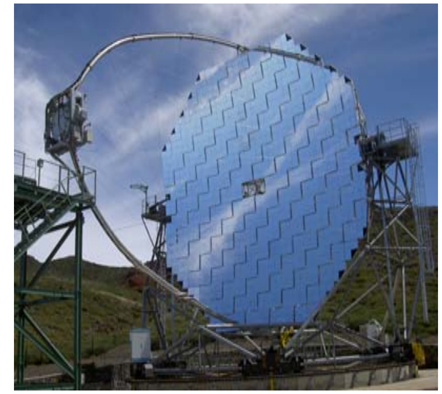

(http://wwwmagic.mppmu.mpg.de/)

QE curves

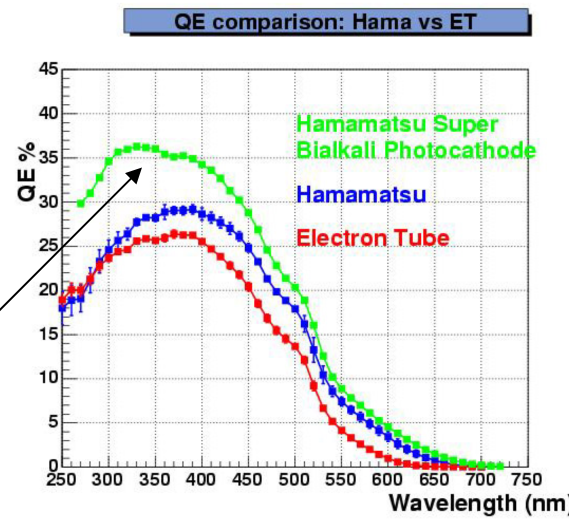

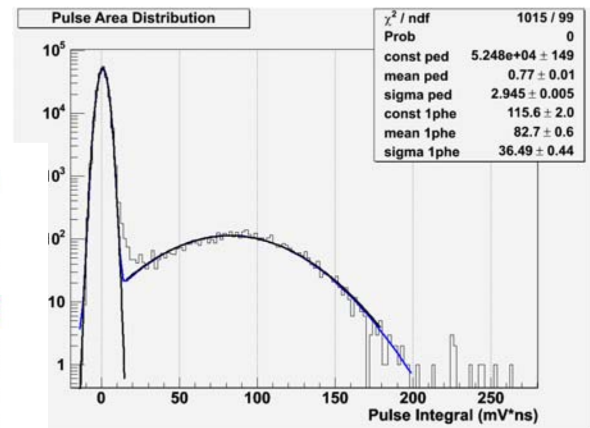

Single PE spectrum

Very High QE HPDs with a GaAsP Photocathode for the MAGIC Telescope Project – T. Saito – P128

- **HPD specifications**
  - GaAsP PC: very high QE ⇒ telescope energy threshold halved
  - APD with T effect compensation (thermistor) for the gain
  - Multi photon counting capability
  - Fast pulse: <1ns rise time
  - Ageing tests: 20% degradation with 300MHz photon background – 1000h/year for 10 years
  - 300 times lower afterpulsing rate than currently-used PMT

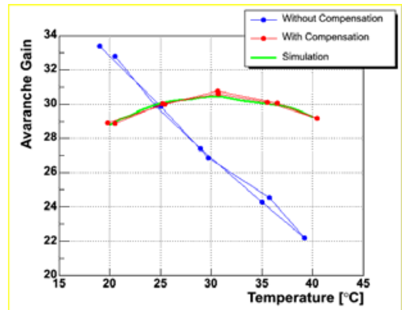

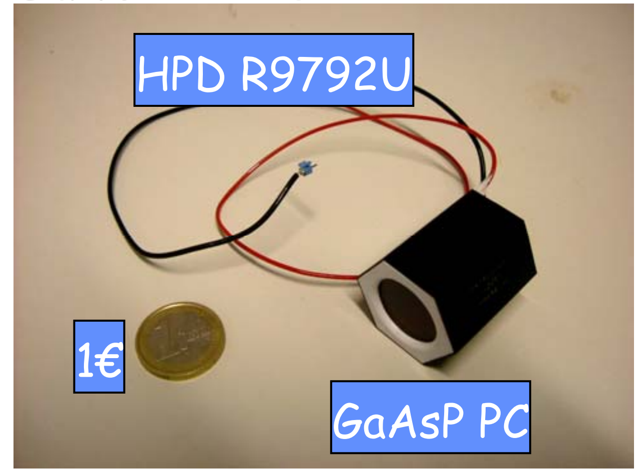

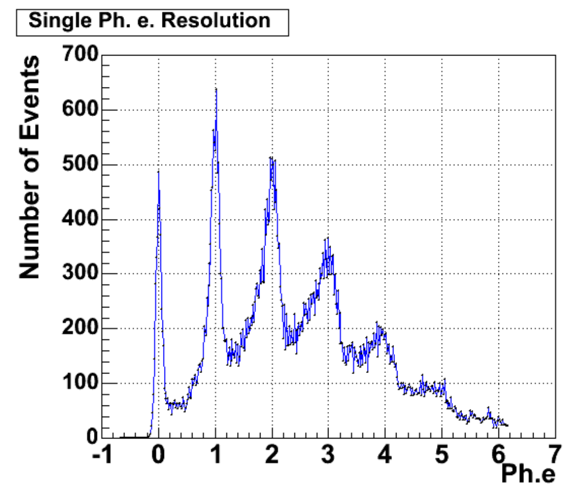

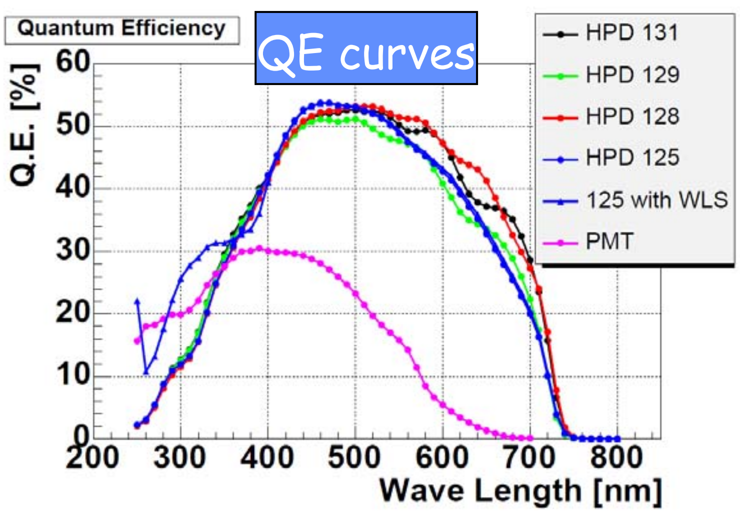

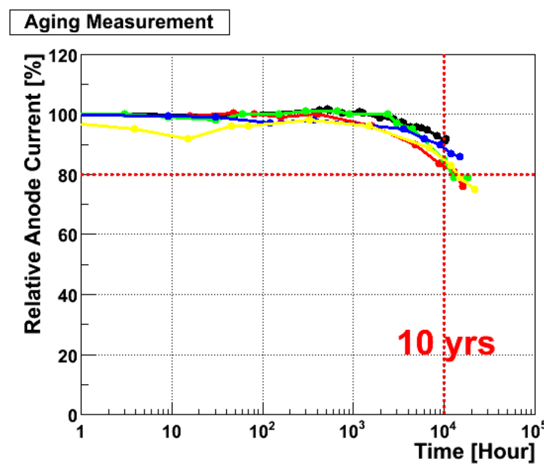

Performance of photomultiplier tubes for cryogenic applications
V. Gallo et al. – P232

- **Dark matter WArP experiment**
  - Inner bi-phasic TPC, outer veto, both filled with LAr (GAr) @ 87K.
  - WIMP-nucleus elastic scattering: 2 ionization signals S1 (prompt) and S2 (ionization e-) @ 128nm shifted to 420nm
- **PMTs**
  - Bi-alkali PC with Pt under-layer to decrease ρ @ low T
  - QE≅20% @ 400nm @ low T
  - Materials with low radioactive contamination
- **Tests of >300 PMTs in liquid N_2**
  - Gain, resolution, SNR, DCR
  - Behaviour w. time: exponential decrease of gain with τ~4-5h, otherwise stable.

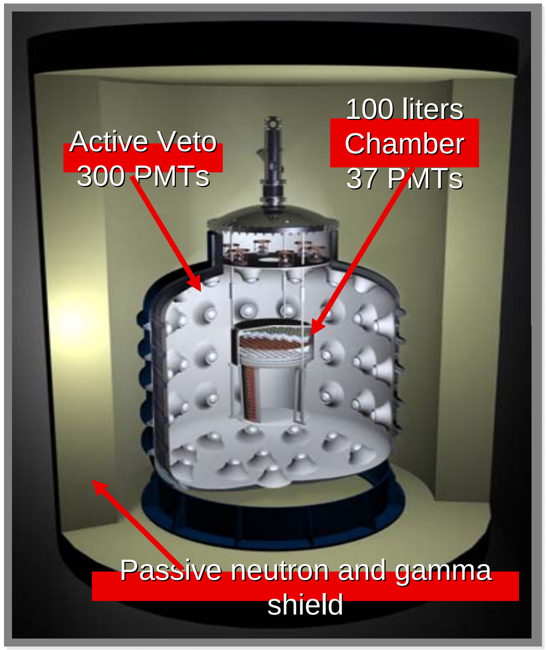

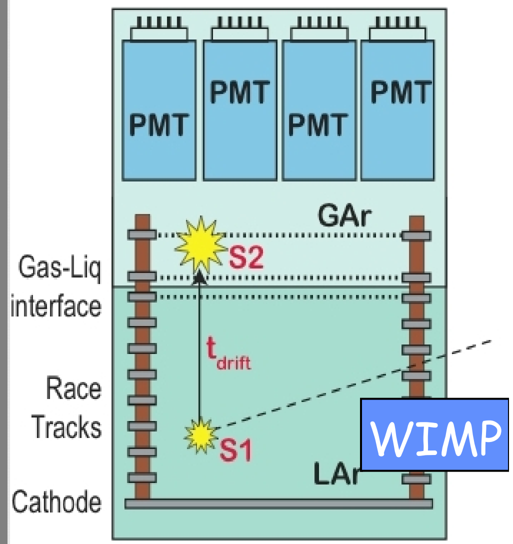

Gain ↓ @ low T

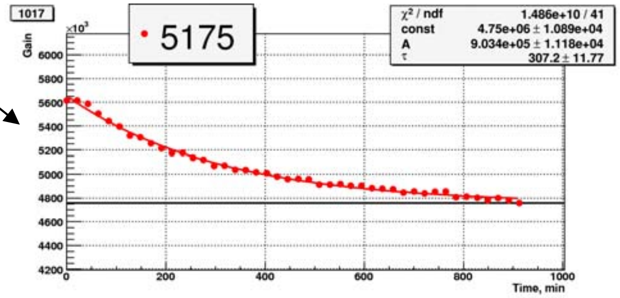

Dark spectrum

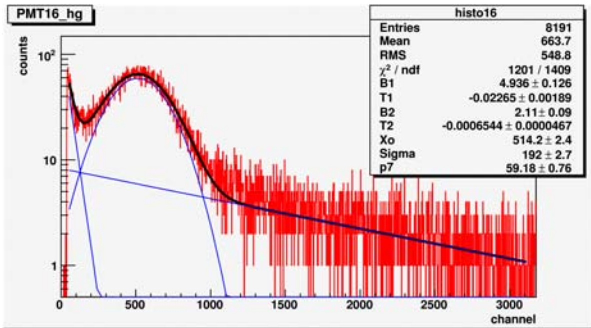

WELCOME TO POSTER SESSION I !

All contributors are looking forward to seeing you in the Poster and Exhibition Hall